Correlation-Driven Lifshitz Transition at the Emergence of the Pseudogap Phase in the Two-Dimensional Hubbard Model

Helena Bragança,[1,2] Shiro Sakai,[3] M. C. O. Aguiar,[1] and Marcello Civelli[2]
[1]Departamento de Física, Universidade Federal de Minas Gerais, C. P. 702, 30123-970 Belo Horizonte, Minas Gerais, Brazil
[2]Laboratoire de Physique des Solides, CNRS UMR 8502, Univ. Paris-Sud, Université Paris-Saclay F-91405 Orsay Cedex, France
[3]Center for Emergent Matter Science, RIKEN, Wako, Saitama 351-0198, Japan

(Received 5 August 2017; published 9 February 2018)

We study the relationship between the pseudogap and Fermi-surface topology in the two-dimensional Hubbard model by means of the cellular dynamical mean-field theory. We find two possible mean-field metallic solutions on a broad range of interactions, doping, and frustration: a conventional renormalized metal and an unconventional pseudogap metal. At half filling, the conventional metal is more stable and displays an interaction-driven Mott metal-insulator transition. However, for large interactions and small doping, a region that is relevant for cuprates, the pseudogap phase becomes the ground state. By increasing doping, we show that a first-order transition from the pseudogap to the conventional metal is tied to a change of the Fermi surface from hole- to electronlike, unveiling a correlation-driven mechanism for a Lifshitz transition. This explains the puzzling link between the pseudogap phase and Fermi surface topology that has been pointed out in recent experiments.

DOI: 10.1103/PhysRevLett.120.067002

In order to understand superconductivity [1–3], one must first understand the normal metallic state, appearing above a critical temperature (T_c), from which it takes its roots. The high-T_c superconductivity in cuprates remains unsolved, mainly because its normal metallic state, the pseudogap (PG) phase, has not been well understood. It has therefore been a central issue to establish the origin of the pseudogap and its relationship with the high-T_c superconducting mechanism [4]. The PG has been revealed [5,6] in spectroscopic responses [7], and thermodynamic and transport properties [8], by a loss of spectral weight, which departs from the conventional Fermi liquid (FL) theory of metals [9,10]. Recent experiments have pointed out that when a Lifshitz transition [i.e., a change of Fermi Surface (FS) topology from electronlike (e) to holelike (h)] is tuned in the PG phase of a cuprate material, the PG ends abruptly. This takes place, for instance, at a doping p^* on the overdoped region of $Bi_2Sr_2CuO_{6+\delta}$ [11], $Bi_2Sr_2CaCu_2O_{8+\delta}$ [12,13], and in $La_{1.6-x}Nd_{0.4}Sr_xCuO_4$ [14]. This finding has been strongly debated, as it challenges our current understanding of the PG phase [4] and its relationship with superconductivity.

Here we give a rational explanation to all of these observations within the framework of the two-dimensional Hubbard model, solved with the cellular dynamical mean-field theory (CDMFT) [15–17]. We first show that two metallic solutions exist: a rather regular correlated Fermi-liquid metal (CFM), and a PG metal (PGM) that violates Fermi-liquid theory by developing a pole divergence in the self-energy. This result could account for contradicting reports about the existence of the Mott metal-insulator transition (MIT) at half filling (zero doping) in two dimensions. The PGM is metastable at weak interactions, having higher energy than the CFM. However, by increasing the interaction at low doping (the region relevant for underdoped cuprates), the PGM emerges as the stable phase, up to the doping value p^*. This is consistent with the CDMFT results of Sordi *et al.* [18]. Most importantly, we show that the PGM is bound to always have a h-FS. The CFM instead can undergo a Lifshitz transition at a doping p_{lt}. However, for a strong interaction, the CFM is stable only for doping $p > p_{lt}$; i.e., it has always an e-FS. Hence, the transition from the PGM to the CFM at p^* is accompanied by a corresponding change from a h-FS to an e-FS, unveiling a novel correlation-driven mechanism of the Lifshitz transition. These results explain why the PG must sharply end when a Lifshitz transition occurs [11], or is tuned by pressure [14], in cuprates.

We consider the two-dimensional one-band Hubbard model:

$$\mathcal{H} = -\sum_{\mathbf{k}\sigma} \xi_{\mathbf{k}} c^{\dagger}_{\mathbf{k}\sigma} c_{\mathbf{k}\sigma} + U \sum_i n_{i\uparrow} n_{i\downarrow}, \tag{1}$$

where $c_{\mathbf{k}\sigma} = (1/\sqrt{L}) \sum_i \exp(-i\mathbf{k}\cdot\mathbf{r}_i) c_{i,\sigma}$ destroys an electron with spin σ and momentum $\mathbf{k}$, $n_{i\sigma} = c^{\dagger}_{i\sigma} c_{i\sigma}$ is the density operator on site i of a L-site square lattice. $\xi_{\mathbf{k}} = -2t(\cos k_x + \cos k_y) - 4t' \cos k_x \cos k_y - \mu$, where t (t') is the (next) nearest-neighbor-site hopping integral, and μ is the chemical potential controlling the doping level $p = 1 - (1/L)\sum_{i,\sigma} \langle n_{i\sigma} \rangle$. We implement the CDMFT at zero temperature ($T = 0$) using Lanczos. This maps $\mathcal{H}$ onto

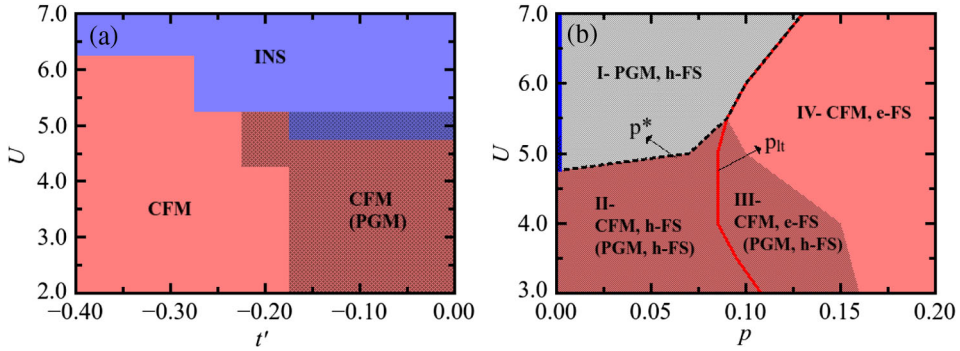

FIG. 1. (a) $U - t'$ phase diagram for the normal state of the two-dimensional Hubbard model at half filling ($p = 0$). The blue, pink, and dark regions bound, respectively, a Mott insulator (INS), a correlated Fermi-liquid metal (CFM), and a coexisting pseudogap metal (PGM). The CFM always has lower energy than the PGM (in parenthesis). (b) $U - p$ phase diagram with $t' = -0.1$. The blue vertical line at $p = 0$ is the INS. The continuous red line p_{lt} marks a Lifshitz transition, where the FS topology changes from electronlike (e-FS) to holelike (h-FS). The dashed black line p^* marks the boundary where the PGM energy becomes higher than the CFM one.

a 2×2 cluster coupled to an 8-site bath [19–21] (see Sec. I of the Supplemental Material (SM) [22]). The numerical calculation provides the frequency dependent Green's function in the corner points of the first quadrant of the Brillouin zone (BZ). To obtain the lattice quantities in momentum space, we perform a periodization based on the cumulant [23–25]. We calculate the total energy as described in Ref. [26] and in Sec. II of the SM, which includes Ref. [27]. We set $t = 1$ and explore the paramagnetic phase diagram in the $U - t'$ space at half filling [Fig. 1(a)], and the $U - p$ space at fixed $t' = -0.1$ [Fig. 1(b)]. At $T = 0$, the ground state is the broken symmetry phase: antiferromagnetism at half filling and small doping, and superconductivity upon doping. These phases have been widely studied within CDMFT [16–18,28–33]. Here we focus on the paramagnetic solution which, albeit being the normal-state ground state only at $T > T_c$, is the mean-field phase from which broken orders take roots. This allows us to study the FS topology and its relationship with the pseudogap.

We start with the half filled system [Fig. 1(a)]. A relevant question is whether in two dimensions a gap is present in the paramagnetic solution at any small U, like in one dimension [34], and as it was proposed by P. W. Anderson [35], or whether the system becomes a regular metal under a critical U_c, i.e., there is a Mott MIT, like in infinite dimensions [36]. This issue has been considered by various groups using quantum cluster methods [37–42], but it has not been completely clarified. In these studies, it was considered the particle-hole symmetric $t' = 0$ case, which is especially singular because a $\mathbf{k} = (\pi, \pi)$ nesting vector acts on the whole FS producing divergent susceptibilities. It is very likely then that at $T = 0$ a gap always opens in the system. To verify Anderson's conjecture we have considered $t' \neq 0$. Our main result is that, for $U < U_c$, we find two different metallic solutions, the CFM and the PGM, as it is shown in Fig. 1(a). The PGM coexists with the CFM for a broad range of U and t' values, disappearing only for large $|t'|$. For an interaction greater than $U \simeq 5t$, we recover the well-known Mott insulating phase. We shall now show that the CFM is the FL solution displaying the Mott transition, in agreement with the statements of publications [37–39,42], while the PGM solution always presents a gap in the spectra reminiscent of the solution found in the works of Refs. [40,41].

For this purpose, we set $t' = -0.1$ and display in Fig. 2 the spectral function $A(\mathbf{k}, \omega) = -(1/\pi)\mathrm{Im}G(\mathbf{k}, \omega)$ and the imaginary part of the self-energy $\mathrm{Im}\Sigma(\mathbf{k}, \omega)$ at $\mathbf{k} = (0, \pi)$, close to the Fermi level ($|\omega| < 0.8t$) (see SM Sec. III for a broader ω range, including the Hubbard bands). The CFM (red-dotted curve) displays typical features of a FL: a finite spectral peak at the Fermi level $\omega = 0$ [Fig. 2(a)] and $\sim\omega^2$ behavior in $\mathrm{Im}\Sigma$ [Fig. 2(b)]. The PGM (black-solid curve) displays sharply distinct features. $A(\mathbf{k}, \omega)$ has a minimum

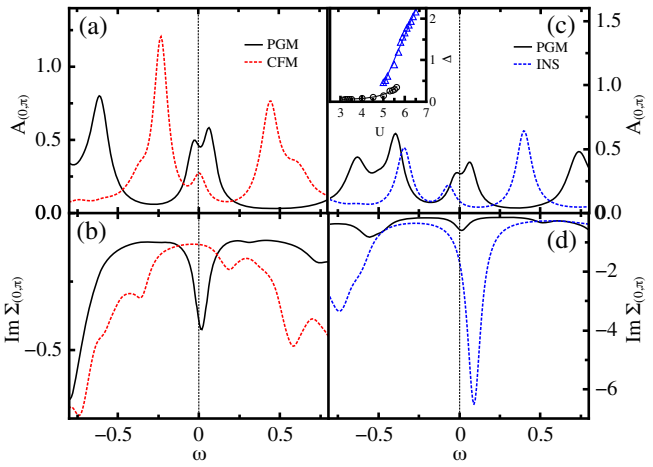

FIG. 2. Low-energy spectral function $A(\mathbf{k}, \omega)$ (a) at $\mathbf{k} = (0, \pi)$ and corresponding imaginary part of the self-energy $\mathrm{Im}\Sigma(\mathbf{k}, \omega)$ (b) of the two coexisting CFM and PGM at half filling, $U = 4.0$, $t' = -0.1$. A comparison of $A(\mathbf{k}, \omega)$ (c) and $\mathrm{Im}\Sigma(\mathbf{k}, \omega)$ (d) between the PGM and the Mott insulator for $U = 5.0$, $t' = -0.1$. Inset: The spectral gap of $A(\mathbf{k}, \omega)$ as a function of U for the PGM (circles) and the Mott insulator (triangles).

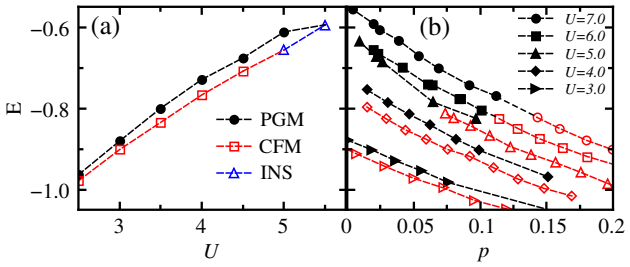

FIG. 3. Total energy E (a) as a function of the interaction at half filling and (b) as a function of doping, both for $t' = -0.1$. Red-open symbols correspond to the CFM solution, while black-filled ones represent the PGM.

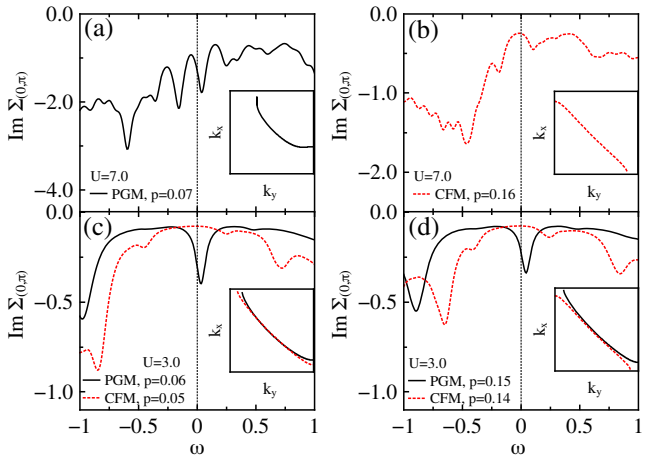

FIG. 4. Comparison of the imaginary part of the self-energy at the antinodal point $\mathbf{k} = (0, \pi)$, between CFM and PGM solutions in various regions [(a) region I, (b) IV, (c) II, (d) III] of the $U - p$ phase diagram of Fig. 1. Inset displays the corresponding FS in the first quadrant of the BZ (k_x, $k_y \in [0, \pi]$).

at $\omega = 0$ [Fig. 2(a)], showing a small gap Δ, which we plot in the inset of Fig. 2(c) (circles) as a function of U, together with the insulator gap (triangles). ImΣ displays a polelike divergence [Fig. 2(b)], which breaks the FL. This behavior of the self-energy is similar to what is expected in a Mott insulator [blue-dotted curve in Fig. 2(d)], whose gap is always characterized by a pole in the self-energy, though in the PGM, the intensity of the divergence is reduced and the two solutions are not smoothly connected, showing a coexistence region [inset of Fig. 2(c)].

We find that at half filling and a different t', the CFM always shows a lower energy than the PGM, as displayed in Fig. 3(a). This validates the concept of Mott MIT, which is also in the two-dimensional Hubbard model (see SM for the kinetic and potential energies). The unstable PGM remains, reminiscent of Anderson's RVB theory [35,43], though relevant differences have been already pointed out [44].

However, the PGM can become the relevant lowest-energy phase upon doping. In the $U - p$ phase diagram of Fig. 1(b), where $t' = -0.1$, we can clearly identify three regions: The PGM (I), the CFM (IV), and a coexisting CFM-PGM region (II and III). In this latter case [see Fig. 3(b) for $U = 3, 4$], the CFM always has the lowest total energy. For $U > U_c \simeq 5t$, at small doping (region relevant for underdoped cuprates), the PGM emerges as the stable solution, while the CFM persists at high dopings. These results are consistent with those of Refs. [18,45], which show a small first-order coexistence region between regions I and IV, which closes at a tricritical point and become continuous for $U \geq 7t$. We think that our Lanczos-implementation has difficulty entering into this small coexistence region, and we cannot say if the transition becomes second order for $U \geq 7t$. However, the first-order character of the transition in the region that we considered is shown by the fact that the PGM and the CFM are not smoothly connected.

In the doped system, we confirm the key physical properties differentiating the CFM and PGM phases, established for half filling. Namely, the PGM always breaks the FL displaying a peak in ImΣ [see Figs. 4(a), 4(c), and 4(d)], which has now moved slightly to a positive frequency. On the other hand, the CFM phase is FL-like on all the phase diagram, displaying a well behaved ω^2 dependence of ImΣ [Fig. 4(b), (c), (d)].

Let us now discuss the implications of these findings in the context of the PG phase of cuprates and its relationship with the FS topology. This has been the subject of pioneering studies [18,23,30,31,46–52], though the physical mechanism at the origin of this relationship has remained not well clarified. The first crucial observation is that the pole in the self-energy in the PGM solution strongly enhances the scattering in the neighborhood of $\mathbf{k} = (0, \pi)$ (antinodes in cuprates). As a consequence, the spectral weight on the FS around $\mathbf{k} = (0, \pi)$ is strongly suppressed, giving a point of origin to the well-known break of the FS into arcs. This can be shown in the spectral function $A(\mathbf{k}, \omega = 0)$ plotted in Fig. 5(a), (c). These results are consistent with previous CDMFT studies [30,47,53] and well describe the angle-resolved photoemission spectroscopy measurements on cuprates [7]. The CFM does not show any Fermi arc [Fig. 5(b), (d)], rather the spectral intensity is enhanced at the antinodes because of the proximity to a van Hove singularity.

The second crucial observation (insets of Fig. 4) is that the *PGM solution always has a h*-FS. To get some insight into this issue, we notice that in the PGM the low-frequency pole in the self-energy can be well-described by $\Sigma(\mathbf{k}, \omega) \simeq V^2/(\omega - \xi^f_{\mathbf{k}})$. This expression has been derived in the framework of a low-energy model called a "hidden fermion" [44,54], but it has also been proposed by complementary approaches to the PG phase of cuprates [48,55–57]. $\xi^f_{\mathbf{k}}$ is located slightly above the Fermi energy in the antinodal region. We see then that, if $\mathbf{k}_F$ is the Fermi wave vector of the noninteracting system located on the $(0, \pi) - (\pi, \pi)$ side of the BZ, such that $\xi_{\mathbf{k}_F} = 0$, the

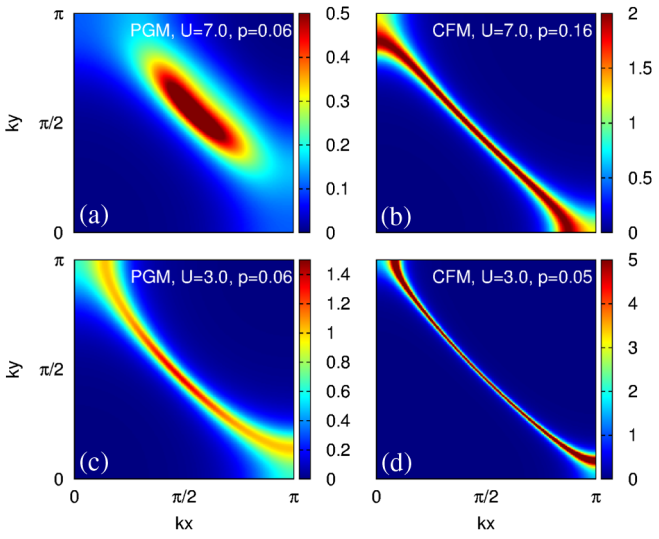

FIG. 5. Spectral function $A(\mathbf{k}, \omega = 0)$ in the first quadrant of the BZ for the CFM and the PGM. At weak interaction $U = 3$ and small doping $p = 0.05$, the underlying FS is holelike in both solutions. In this case, however, the CFM is the stable solution, not showing Fermi arcs. At strong interaction $U = 7.0$, the PGM is stable at small doping ($p = 0.06$), displaying Fermi arcs and a h-FS, while the CFM is stable at high doping ($p = 0.16$), displaying no arc and an e-FS.

polelike singularity of the self-energy in the interacting system acts in such a way that the new Fermi wave vector $\mathbf{k}'_F$ is given by $\xi_{\mathbf{k}'_F} - V^2/\xi^f_{\mathbf{k}'_F} = 0$. If $\xi^f_{\mathbf{k}'_F}$ is positive as it is for $\mathbf{k} = (0, \pi)$, it acts as an enhanced chemical potential (see SM Sec. IV) and $\mathbf{k}'_F > \mathbf{k}_F$; i.e., the interacting FS is *more holelike*. To undergo a transition from the h-FS to the e-FS in the PGM, the FS must cross the $\mathbf{k} = (0, \pi)$ point, but this is preempted by the pole singularity of the self-energy. One possibility is to have the pole singularity position $\xi^f_{\mathbf{k}}$ move to negative frequencies. As noticed in Ref. [49], this can be achieved by tuning t' to positive values, which is equivalent to consider electron-doped cuprates, as the same tuning can be realized by a particle-hole transformation of the Hamiltonian (1) that changes the sign of t' [53]. Another possibility is to have the pole singularity disappear ($V \to 0$), but in this case, one loses the PGM solution. We then establish an indissoluble tight relationship within the PGM solution between the pole in the self-energy, the PG, and the holelike FS.

Putting it all together, we provide a rational understanding to the experimental observations that the PG ending point is linked to a Lifshitz transition, and above all, why this appears first order [12,13], or at least very sharp [11,14], in experiments. Starting from a weak U [see Fig. 1(b)], the stable solution is the CFM, which by increasing doping, presents a renormalized [49] Fermi liquidlike Lifshitz transition at $p = p_{lt}$ [continuous red line in Fig. 1(b)], where one goes continuously from a h-FS to an e-FS. There is no PG in this case; the PG is present in the PGM, which has a h-FS [Fig. 5(c)], but this phase is unstable. When the p_{lt} boundary on the $U - p$ phase diagram meets the PGM-CFM transition boundary p^* (black-dashed lines) at the stronger $U \simeq 5.5t$, we find for $p < p^*$ the PGM as the stable solution, which has a h-FS, while for $p > p^*$, the CFM is the stable solution, but this already has an e-FS [Fig. 5(b)]. By increasing p, the change from h-FS to e-FS is *bound* to the PGM-CFM phase transition ($p_{lt} \equiv p^*$), which is first order, providing a correlated mechanism for the Lifshitz transition. This is consistent with the experimental observations in Bi-based [11–13] and La-based compounds [14]. On the other hand, there is a region of the phase diagram in the range $4.5t < U < 5.5t$, where the PGM-CFM transition takes place at a doping smaller than the Lifshitz transition of the CFM solution; i.e., $p^* < p_{lt}$. At p^*, the PG disappears, but the FS is still holelike. This may account for the Tl-based [58,59] and Y-based [60] cuprates, which have been reported to have a h-FS but no PG. This may also crucially depend on the $|t'/t|$ value, as pointed out in Ref. [49]. Our paramagnetic CDMFT phase diagram of the two-dimensional Hubbard model can then fully account for apparently contradicting and debating experimental results on different members of the cuprate family, showing that there truly exists a tight relationship between PG and FS topology. This should manifest itself in cuprates whenever a Lifshitz transition takes place in the pseudogap phase.

In conclusion, we have studied the paramagnetic normal state of the two-dimensional Hubbard model at zero temperature for a broad range of interaction, U, frustration, t', and doping level, p. Our main finding is the coexistence of a correlated Fermi liquid metal (CFM) with a non-Fermi liquid metal (PGM). At half filling, we answer an open debate by showing that the CFM is the stable solution and displays a correlation-driven Mott MIT differently from the PGM, which instead displays a PG in the spectra. Next, we show that for strong interactions and small doping, a region relevant for underdoped cuprates, the PGM becomes the stable solution. This result is at the origin of a correlation-driven Lifshitz transition, as by increasing doping, a first-order transition takes place from the PGM phase, which has a h-FS, to the CFM, which at these interaction values has an e-FS. Our theory rationalizes the variety displayed on the phase diagram of the cuprate family, telling us that if the PG meets a Lifshitz transition, then it should collapse. This also implies that the PG cannot exists on an e-FS. The behavior of the PG that is sensitive to the FS topology must be contrasted with the one of superconductivity, which does not appear much affected by the Lifshitz transition [13]. This may represent the key to finally unveiling the true nature of the relationship between the PG and the high-T_c mechanism. Future experimental and theoretical investigations should be pursued in this direction.

During our investigations, we became aware of the work of Ref. [49], whose results are in good agreement with ours.

Our PGM, however, is found as a second metastable solution distinct from the CFM. This, in particular, discloses the origin of the tight link between the PG and the correlated first-order Lifshitz transition.

We thank I. Paul for his insightful comments. We acknowledge discussion with W. Wu, M. Ferrero, A. Georges, B. Loret, A. Sacuto, O. Parcollet, A.-M. Tremblay, and G. Sordi. This work was supported by CNPq, CAPES and FAPEMIG, and Grants JSPS KAKENHI (No. 16H06345 and No. 17K14350), support from the INCT on Quantum Information/CNPq is also gratefully acknowledged. Part of the results were obtained at CENAPAD-SP.

[1] J. Bardeen, L. N. Cooper, and J. R. Schrieffer, Microscopic theory of superconductivity, Phys. Rev. **106**, 162 (1957).
[2] A. B. Migdal, Interaction between electrons and lattice vibrations in a normal metal, J. Exp. Theor. Phys. **7**, 996 (1958).
[3] G. M. Eliashberg, Interactions between electrons and lattice vibrations in a superconductor, J. Exp. Theor. Phys. **11**, 696 (1960).
[4] M. Norman, D. Pines, and C. Kallin, The pseudogap: Friend or foe of high T_c? Adv. Phys. **54**, 715 (2005).
[5] H. Alloul, T. Ohno, and P. Mendels, ^{89}Y NMR Evidence for a Fermi-Liquid Behavior in $YBa_2Cu_3O_{6+x}$, Phys. Rev. Lett. **63**, 1700 (1989).
[6] W. W. Warren, R. E. Walstedt, G. F. Brennert, R. J. Cava, R. Tycko, R. F. Bell, and G. Dabbagh, Cu Spin Dynamics and Superconducting Precursor Effects in Planes Above Tc in $YBa_2Cu_3O_{6.7}$, Phys. Rev. Lett. **62**, 1193 (1989).
[7] A. Damascelli, Z. Hussain, and Z.-X. Shen, Angle-resolved photoemission studies of the cuprate superconductors, Rev. Mod. Phys. **75**, 473 (2003).
[8] T. Timusk and B. Statt, The pseudogap in high-temperature superconductors: An experimental survey, Rep. Prog. Phys. **62**, 61 (1999).
[9] A. A. Abrikosov, L. P. Gorkov, and I. E. Dzyaloshinski, *Methods of Quantum Field Theory in Statistical Mechanics* (Dover, New York, 1963).
[10] P. Nozières, *Interacting Fermi Systems* (Benjamin, New York, 1964).
[11] A. Piriou, N. Jenkins, C. Berthod, I. Maggio-Aprile, and O. Fischer, First direct observation of the Van Hove singularity in the tunnelling spectra of cuprates, Nat. Commun. **2**, 221 (2011).
[12] S. Benhabib, A. Sacuto, M. Civelli, I. Paul, M. Cazayous, Y. Gallais, M.-A. Measson, R. D. Zhong, J. Schneeloch, G. D. Gu, D. Colson, and A. Forget, Collapse of the Normal State Pseudogap at a Lifshitz Transition in $Bi_2Sr_2CaCu_2O_{8+\delta}$ Cuprate Superconductor, Phys. Rev. Lett. **114**, 147001 (2015).
[13] B. Loret, S. Sakai, S. Benhabib, Y. Gallais, M. Cazayous, M. A. Measson, R. D. Zhong, J. Schneeloch, G. D. Gu, A. Forget, D. Colson, I. Paul, M. Civelli, and A. Sacuto, Vertical temperature-boundary of the pseudogap under the superconducting dome of the $Bi_2Sr_2CaCu_2O_{8+d}$ phase-diagram, Phys. Rev. B **96**, 094525 (2017).
[14] N. Doiron-Leyraud, O. Cyr-Choinière, S. Badoux, A. Ataei, C. Collignon, A. Gourgout, S. Dufour-Beauséjour, F. F. Tafti, F. Laliberté, M. Matusiak, D. Graf, M. Kim, J.-S. Zhou, N. Momono, T. Kurosawa, H. Takagi, and L. Taillefer, Pseudogap phase of cuprate superconductors confined by Fermi surface topology, Nat. Commun. **8**, 2044 (2017).
[15] G. Kotliar, S. Y. Savrasov, G. Pálsson, and G. Biroli, Cellular Dynamical Mean Field Approach to Strongly Correlated Systems, Phys. Rev. Lett. **87**, 186401 (2001).
[16] T. Maier, M. Jarrell, T. Pruschke, and M. H. Hettler, Quantum cluster theories, Rev. Mod. Phys. **77**, 1027 (2005).
[17] A.-M. S. Tremblay, B. Kyung, and D. Sénéchal, Pseudogap and high-temperature superconductivity from weak to strong coupling. Towards a quantitative theory. J. Low Temp. Phys. **32**, 424 (2006).
[18] G. Sordi, K. Haule, and A.-M. S. Tremblay, Finite Doping Signatures of the Mott Transition in the Two-Dimensional Hubbard Model, Phys. Rev. Lett. **104**, 226402 (2010).
[19] M. Civelli, The doping-driven evolution of the superconducting state of a doped Mott insulator: a key for the high temperature superconductivity, Phys. Rev. B **79**, 195113 (2009).
[20] M. Capone, M. Civelli, S. S. Kancharla, C. Castellani, and G. Kotliar, Cluster-dynamical mean-field theory of the density-driven Mott transition in the one-dimensional Hubbard model, Phys. Rev. B **69**, 195105 (2004).
[21] M. Civelli, Ph.D. thesis, Rutgers University, Piscataway, 2006, arXiv:0710.2802.
[22] See Supplemental Material at http://link.aps.org/supplemental/10.1103/PhysRevLett.120.067002 for more details about the numerical calculation.
[23] T. D. Stanescu and G. Kotliar, Fermi arcs and hidden zeros of the Green function in the pseudogap state, Phys. Rev. B **74**, 125110 (2006).
[24] T. D. Stanescu, M. Civelli, K. Haule, and G. Kotliar, A cellular dynamical mean field theory approach to Mottness, Ann. Phys. (Amsterdam) **321**, 1682 (2006).
[25] S. Sakai, G. Sangiovanni, M. Civelli, Y. Motome, K. Held, and M. Imada, Cluster-size dependence in cellular dynamical mean-field theory, Phys. Rev. B **85**, 035102 (2012).
[26] E. Gull and A. J. Millis, Energetics of superconductivity in the two dimensional Hubbard model, Phys. Rev. B **86**, 241106(R) (2012).
[27] G. D. Mahan, *Many-Particle Physics*, 3rd ed. (Kluwer Academic/Plenum Publishers, New York, 2000).
[28] G. Kotliar, S. Y. Savrasov, K. Haule, V. S. Oudovenko, O. Parcollet, and C. A. Marianetti, Electronic structure calculations with dynamical mean-field theory, Rev. Mod. Phys. **78**, 865 (2006).
[29] S. S. Kancharla, B. Kyung, D. Sénéchal, M. Civelli, M. Capone, G. Kotliar, and A.-M. S. Tremblay, Anomalous superconductivity and its competition with antiferromagnetism in doped Mott insulators, Phys. Rev. B **77**, 184516 (2008).
[30] M. Ferrero, P. S. Cornaglia, L. De Leo, O. Parcollet, G. Kotliar, and A. Georges, Pseudogap opening and formation of Fermi arcs as an orbital-selective Mott transition in momentum space, Phys. Rev. B **80**, 064501 (2009).

[31] E. Gull, M. Ferrero, O. Parcollet, A. Georges, and A. J. Millis, Momentum space anisotropy and pseudogaps: A comparative cluster dynamical mean field analysis of the doping-driven metal-insulator transition in the two dimensional Hubbard model, Phys. Rev. B **82**, 155101 (2010).
[32] E. Gull, O. Parcollet, and A. J. Millis, Superconductivity and the Pseudogap in the Two-Dimensional Hubbard Model, Phys. Rev. Lett. **110**, 216405 (2013).
[33] E. Gull and A. J. Millis, Quasiparticle properties of the superconducting state of the two-dimensional Hubbard model, Phys. Rev. B **91**, 085116 (2015).
[34] E. H. Lieb and F. Y. Wu, Absence of Mott Transition in an Exact Solution of the Short-Range, One-Band Model in One Dimension, Phys. Rev. Lett. **20**, 1445 (1968).
[35] P. W. Anderson, *The Theory of Superconductivity in the High-Tc Cuprates* (Princeton University Press, Princeton, 1997).
[36] A. Georges and G. Kotliar, Hubbard model in infinite dimensions, Phys. Rev. B **45**, 6479 (1992).
[37] Y. Z. Zhang and M. Imada, Pseudogap and Mott transition studied by cellular dynamical mean field theory, Phys. Rev. B **76**, 045108 (2007).
[38] H. Park, K. Haule, and G. Kotliar, Cluster Dynamical Mean Field Theory of the Mott Transition, Phys. Rev. Lett. **101**, 186403 (2008).
[39] M. Balzer, B. Kyung, D. Sénéchal, A.-M. S. Tremblay, and M. Potthoff, First order Mott transition at zero temperature in two dimensions: Variational plaquette study, Europhys. Lett. **85**, 17002 (2009).
[40] S. Moukouri and M. Jarrell, Absence of a Slater Transition in the Two-Dimensional Hubbard Model, Phys. Rev. Lett. **87**, 167010 (2001).
[41] T. Schäfer, F. Geles, D. Rost, G. Rohringer, E. Arrigoni, K. Held, N. Blümer, M. Aichhorn, and A. Toschi, Fate of the false Mott-Hubbard transition in two dimensions, Phys. Rev. B **91**, 125109 (2015).
[42] L. Fratino, P. Sémon, M. Charlebois, G. Sordi, and A.-M. S. Tremblay, Signatures of the Mott transition in the antiferromagnetic state of the two-dimensional Hubbard model, Phys. Rev. B **95**, 235109 (2017).
[43] L. F. Tocchio, F. Becca, and S. Sorella, Hidden Mott transition and large-U superconductivity in the two-dimensional Hubbard model, Phys. Rev. B **94**, 195126 (2016).
[44] S. Sakai, M. Civelli, and M. Imada, Evidence for Hidden Fermion that Triggers High-Temperature Superconductivity in Cuprates, Phys. Rev. Lett. **116**, 057003 (2016).
[45] J. P. L. Faye and D. Sénéchal, Pseudogap to metal transition in the anisotropic two-dimensional Hubbard model, Phys. Rev. B **96**, 195114 (2017).
[46] A. Liebsch and N.-H. Tong, Finite-temperature exact diagonalization cluster dynamical mean-field study of the two-dimensional Hubbard model: Pseudogap, non-Fermi-liquid behavior, and particle-hole asymmetry, Phys. Rev. B **80**, 165126 (2009).
[47] S. Sakai, Y. Motome, and M. Imada, Evolution of Electronic Structure of Doped Mott Insulators: Reconstruction of Poles and Zeros of Green's Function, Phys. Rev. Lett. **102**, 056404 (2009).
[48] K.-Y. Yang, T. M. Rice, and F.-C. Zhang, A phenomenological theory of the pseudogap state, Phys. Rev. B **73**, 174501 (2006).
[49] W. Wu, M. S. Scheurer, S. Chatterjee, S. Sachdev, A. Georges, and M. Ferrero, Pseudogap and Fermi surface topology in the two-dimensional Hubbard model, arXiv:1707.06602.
[50] K.-S. Chen, Z. Y. Meng, T. Pruschke, J. Moreno, and M. Jarrell, Lifshitz transition in the two-dimensional Hubbard model, Phys. Rev. B **86**, 165136 (2012).
[51] D. Sénéchal and A.-M. S. Tremblay, Hot Spots and Pseudogaps for Hole- and Electron-Doped High-Temperature Superconductors, Phys. Rev. Lett. **92**, 126401 (2004).
[52] Th. A. Maier, Th. Pruschke, and M. Jarrell, Angle-resolved photoemission spectra of the Hubbard model, Phys. Rev. B **66**, 075102 (2002).
[53] M. Civelli, M. Capone, S. S. Kancharla, O. Parcollet, and G. Kotliar, Dynamical Breakup of the Fermi Surface in a Doped Mott Insulator, Phys. Rev. Lett. **95**, 106402 (2005).
[54] M. Imada, Y. Yamaji, S. Sakai, and Y. Motome, Theory of pseudogap and superconductivity in doped Mott insulators, Ann. Phys. (Amsterdam) **523**, 629 (2011).
[55] Y. Yamaji and M. Imada, Composite fermion theory for pseudogap phenomena and superconductivity in underdoped cuprate superconductors, Phys. Rev. B **83**, 214522 (2011).
[56] P. W. Phillips, B. W. Langley, and J. A. Hutasoit, Un-Fermi liquids: Unparticles in strongly correlated electron matter, Phys. Rev. B **88**, 115129 (2013).
[57] C. Morice, X. Montiel, and C. Pépin, Evolution of spectral and transport quantities with doping in the SU(2) theory of cuprates, Phys. Rev. B **96**, 134511 (2017).
[58] M. Platé *et al.*, Fermi Surface and Quasiparticle Excitations of Overdoped $Tl_2Ba_2CuO_{6+\delta}$, Phys. Rev. Lett. **95**, 077001 (2005).
[59] D. C. Peets, J. D. F. Mottershead, B. Wu, I. S. Elfimov, R. Liang, W. N. Hardy, D. A. Bonn, M. Raudsepp, N. J. C. Ingle, and A. Damascelli, $Tl_2Ba_2CuO_{6+d}$ Brings spectroscopic probes deep into the overdoped regime of the high-Tc cuprates, New J. Phys. **9**, 28 (2007).
[60] M. A. Hossain, J. D. F. Mottershead, A. Bostwick, J. L. McChesney, E. Rotenberg, R. Liang, W. N. Hardy, G. A. Sawatzky, I. S. Elfimov, D. A. Bonn, and A. Damascelli, In situ doping control of the surface of high-temperature superconductors, Nat. Phys. **4**, 527 (2008).